# Premorbid Steatohepatitis Increases the Seriousness of Dextran Sulfate Sodium-induced Ulcerative Colitis in Mice

Meng-Yu Wang[1#], Zi-Xuan Wang[1#], Lei-Jie Huang[1], Rui-Xu Yang[1], Zi-Yuan Zou[1], Wen-Song Ge[1], Tian-Yi Ren[1*] and Jian-Gao Fan[1,2*]

[1]Department of Gastroenterology, Xinhua Hospital Affiliated to Shanghai Jiao Tong University School of Medicine, Shanghai, China; [2]Shanghai Key Lab of Pediatric Gastroenterology and Nutrition, Shanghai, China

## Abstract

***Background and Aims:*** The concurrence of nonalcoholic steatohepatitis (NASH) and ulcerative colitis (UC) is increasingly seen in clinical practice, but the underlying mechanisms remain unclear. This study aimed to develop a mouse model of the phenomenon by combining high-fat high-cholesterol diet (HFHCD)-induced NASH and dextran sulfate sodium (DSS)-induced UC, that would support mechanistic studies. ***Methods:*** Male C57BL/6 mice were randomly assigned to two groups receiving either a chow diet or HFHCD for 12 weeks of NASH modeling. The mice were divided into four subgroups for UC modeling: (1) A control group given a chow diet with normal drinking water; (2) A colitis group given chow diet with 2% DSS in drinking water; (3) A steatohepatitis group given HFHCD with normal drinking water; and (4) A steatohepatitis + colitis group given HFHCD with 2% DSS in drinking water. ***Results:*** NASH plus UC had high mortality (58.3%). Neither NASH nor UC alone were fatal. Although DSS-induced colitis did not exacerbate histological liver injury in HFHCD-fed mice, premorbid NASH significantly increased UC-related gut injury compared with UC alone. It was characterized by a significantly shorter colon, more colonic congestion, and a higher histopathological score ($p<0.05$). Inflammatory (tumor necrosis factor-alpha, interleukin 1 beta, C-C motif chemokine ligand 2, and nuclear factor kappa B) and apoptotic (*Bcl2*, *Bad*, *Bim*, and *Bax*) signaling pathways were significantly altered in distal colon tissues collected from mice with steatohepatitis + colitis compared with the other experimental groups. ***Conclusions:*** Premorbid steatohepatitis significantly aggravated DSS-induced colitis and brought about a lethal phenotype. Potential links between NASH and UC pathogeneses can be investigated using this model.

## Introduction

Ulcerative colitis (UC) is one of the two major forms of inflammatory bowel disease (IBD) and presents with a series of immune-mediated gut dysfunctions. UC involves chronic relapsing inflammation of the colon and rectum, and symptoms of diarrhea, abdominal pain, bleeding, and malabsorption.[1] UC occurs across all ages, and the disease burden has been rapidly increasing, especially in newly-industrialized areas.[2,3] Without proper management, such as steroid-based therapies, UC mortality can exceed 50%.[4] The etiology, risk factors, and underlying mechanisms of UC are currently unclear, which necessitates the exploration of novel research tools.[5,6]

Intriguingly, the epidemiology of UC is similar to that of nonalcoholic fatty liver disease (NAFLD). Both are increasing in Western countries, plateauing in certain regions, and gradually spreading to developing areas in parallel with urbanization, industrialization, and relevant environmental changes, especially in lifestyle and diet.[7] Cross-sectional studies demonstrated that up to 40% of IBD patients were overweight or obese, while underweight individuals accounted for no more than 3% of UC patients.[8] A recent meta-analysis estimated NAFLD to be present in approximately 28% of IBD patients, especially in subgroups with severe disease.[9] Despite the observed prevalence of NAFLD among IBD patients, interactions between the two diseases and resulting effects are poorly understood.

Existing evidence linking NAFLD and UC is far from conclusive, but is sufficient to attract research interest. The interplay between gut and liver, the so-called gut-liver axis, may provide a critical piece of the puzzle.[10] The bidirectional communication between gut and liver relies on an anatomical and functional loop including the portal vein, which delivers gut products to liver, and hepatic secretion of bile acids and antibodies, which reflects the feedback route from liver to intestine.[11] Gut dysfunction and dysbiosis are not only the major signs, but also the predominant etiologies of NAFLD. There is

**Table 1. Diet information**

|  | HFHCD | Chow diet |
|---|---|---|
| Energy Source (%) |  |  |
|     Protein | 17% | 20.70% |
|     Fat | 33% | 16.50% |
|     Carbohydrate | 50% | 62.80% |
| Calorie density (kcal/g) | 3.9 | 3.7 |

ample evidence that NAFLD patients have altered gut microbiota composition, bacterial overgrowth, increased intestinal permeability, and an impaired gut-vascular barrier,[12,13] which are also commonly found in UC patients.[14,15] Gut inflammation and pathobiont colonization can promote metabolic and immunologic pathways that boost the overgrowth of dysbiosis species.[16] Evidence from clinical studies indicates that intestinal regions with abundant bacteria are peculiarly prone to UC lesions and that elimination of microbiota disturbances either by fecal diversion or antibiotics might effectively control disease progression.[15] In the liver, hepatocytes secrete primary bile acids, immunoglobulin A, and angiogenin into the gut to modulate the microbiota. The latter convert primary bile acids to secondary bile acids that then circulate back to the liver where they regulate nuclear receptor-mediated activity of glucose metabolism, lipid metabolism, and energy homeostasis.[17] Studies have revealed that the liver releases many inflammatory cytokines and metabolites into the circulation to induce a perpetual state of chronic inflammation during lipid overload.[10,18] Correspondingly, inflammasome-governed modulation of gut microbiota was reported to be a key determinant of both NASH progression and UC pathogenesis.[19,20]

Despite the findings mentioned above, current animal models are somewhat lacking as they do not include interactions between the fatty liver and inflamed intestine. In this study, we introduce a combined mouse model of UC and nonalcoholic steatohepatitis (NASH), a subtype of advanced NAFLD with a NASH phenotype, exacerbated intestinal inflammation, and most importantly, high mortality. We believe that a practical animal model may pave the way for elucidating the potential association and directional progression of NASH and UC.

## Methods

### Animal experiments

Specific pathogen free male C57BL/6 mice, 8 weeks of age, and 20 to 22 g body weight (Shanghai Laboratory Animal Center, Shanghai, China) were maintained under a standard 12 h dark/light cycle with water and chow diet provided ad libitum. After 7 days of acclimatization, mice were randomly assigned to two groups for two different types of diets, chow (*n*=24) or a high-fat high-cholesterol diet (HFHCD) including 88% chow, 10% lard and 2% cholesterol (*n*=28) for 12 weeks. The energy sources and calorie density information of both diets are shown in Table 1. At week 12, six mice were randomly chosen from each group to verify successful NASH modeling, and the remaining mice entered the second phase of modeling. The chow diet group was divided into two subgroups, controls (*n*=8) and colitis (*n*=10). The HFHCD group was also divided into two subgroups, steatohepatitis (*n*=10), and steatohepatitis + colitis (*n*=12). Mice in the colitis and steatohepatitis + colitis groups were challenged with oral dextran sulfate sodium (DSS, 2% in the drinking water). The control and steatohepatitis groups received normal drinking water instead, as previously described.[21] Mice received water with DSS for 1 week and were switched back to normal drinking water and allowed to rest and recover from intestinal injury for the following 2 weeks, which was considered as one round of treatment. During DSS treatment, all mice were still provided with a chow diet or HFHCD as before. After three rounds of DSS treatment, all mice were euthanized by pentobarbital sodium for tissue collection 1 weeks after the last round of DSS treatment (week 20). In short, modeling took a total of 20 weeks and consisted of two modeling phases, 12 weeks for the first phase and 8 weeks for the second phase, as shown in Figure 1. All animal experiments were approved by the Institutional Animal Care and Use Committee of Xinhua hospital affiliated to Shanghai Jiao Tong University School of Medicine and were conducted in accord with the
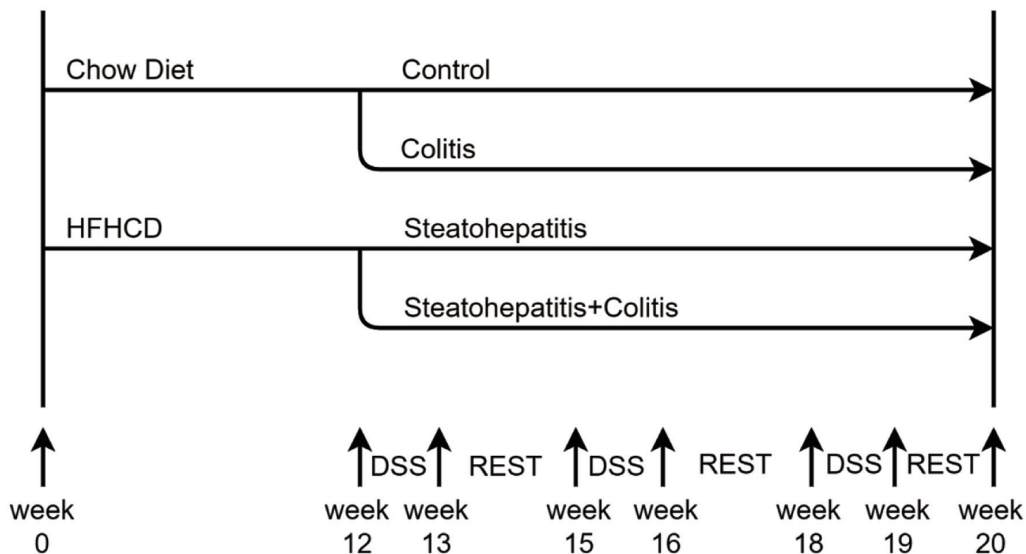


**Fig. 1. Overview of the hybrid model** Male C57bl/6 mice were fed a chow diet or HFHCD for 12 weeks of NASH modeling and were then divided into four subgroups (control, colitis, steatohepatitis, and steatohepatitis + colitis) before being challenged with 2% DSS in drinking water. Normal drinking water was the control). DSS, dextran sulfate sodium; HFHCD, high-fat high-cholesterol diet.

**Table 2. Disease activity index score of colitis**

| Weight loss (%) | Stool property | Rectal bleeding | Score |
|---|---|---|---|
| 0 | Normal | Normal | 0 |
| 1–5 | Soft stool | Stool occult blood | 1 |
| 5–10 | | | 2 |
| 10–15 | Diarrhea | Rectal bleeding | 3 |
| >15 | | | 4 |

**Table 3. qRT-PCR primer sequences**

| Gene | Sequence |
|---|---|
| 18 s | F: GACTCAACACGGGAAACCTCACC |
| | R: ACCAGACAAATCGCTCCACCAAC |
| *Tnfa* | F: CTTCTGTCTACTGAACTTCGGG |
| | R: CAGGCTTGTCACTCGAATTTTG |
| *Il1b* | F: AGAGCCCATCCTCTGTGACTCA |
| | R: TGCTTGGGATCCACACTCTCCA |
| *Ccl2* | F: TTAAAAACCTGGATCGGAACCAA |
| | R: GCATTAGCTTCAGATTTACGGGT |
| *f4/80* | F: ACCACAATACCTACATGCACC |
| | R: AAGCAGGCGAGGAAAAGATAG |
| *Bcl2* | F: GATGACTTCTCTCGTCGCTAC |
| | R: GAACTCAAAGAAGGCCACAATC |
| *Bad* | F: GAAGACGCTAGTGCTACAGATA |
| | R: CTGCTGATGAATGTTGCTCC |
| *Bim* | F: CCCCACTTTTCATCTTTGTGAG |
| | R: TTGTGTTGACTTGTCACAACTC |
| *Bax* | F: TTGCCCTCTTCTACTTTGCTAG |
| | R: CCATGATGGTTCTGATCAGCTC |

guidelines of National Research Council Guide for Care and Use of Laboratory Animals.

### Body composition

Before sacrifice, mice were anesthetized and the body composition was assessed by nuclear magnetic resonance (NMR; Minispec LF50, Bruker Optics, Germany). The total fat and lean body masses were measured by NMR, and body composition was reported as the ratio of total fat mass/body weight and the ratio of total lean mass/body weight.

### Disease activity index (DAI) score of colitis

The severity of colitis was determined daily using the DAI.[22] Specifically, as shown in Table 2, the changes in animal weight loss, rectal bleeding, and presence of diarrhea were assessed on a scale of 0 to 4. The final score was the average value of the three ratings.

### Plasma and tissue assays

Plasma (3,000 rpm centrifugation, 10 m) and liver were obtained and stored at −80°C. Plasma alanine aminotransferase (ALT) and aspartate aminotransferase (AST) were measured using commercially available kits (SSUF, Shanghai, China). Plasma triglycerides, plasma cholesterol, hepatic triglyceride, and hepatic cholesterol levels were measured with assay kits (Applygen Technologies Inc., Beijing, China). Liver samples were weighed, and the liver index was calculated as the ratio between liver weight and body weight. Hepatic lipopolysaccharide (LPS) level was measured using a commercially available assay kit (Servicebio, Wuhan, China).

### Total RNA isolation and real-time quantitative PCR (qRT-PCR)

Total RNA was purified from tissues or cell samples, as previously described.[23] The quality and quantity of RNA samples were verified with a NanoDrop 2000 spectrophotometer (Nanodrop Technologies). cDNA was synthesized using RT master mix (RR036A, Takara, Dalian, China). qRT-PCR was performed with SYBR Green Master Mix (Low Rox Plus, 11202ES08, YEASEN, Shanghai, China). The primer sequences used for qRT-PCR are listed in Table 3.

### Western blotting

Distal colons were snap frozen in liquid nitrogen and stored

at −80°C. Colon proteins were separated by 10% sodium dodecyl sulfate-polyacrylamide gel electrophoresis, and then transferred to polyvinylidene fluoride membranes. The membranes were blocked with Quick Block buffer (Beyotime, Shanghai, China) and incubated with anti-β-Actin antibody (3700, Cell Signal Technology, Danvers, MA, USA), anti-Bax antibody (2772, Cell Signal Technology) and anti-NF-κB p65 antibody (8242, Cell Signal Technology) overnight at 4°C, followed by incubation with the secondary antibodies (Beyotime, Shanghai, China).

### Histological analysis and working definitions

Liver and colon tissues were collected from mice immediately after sacrifice. About 1.0 cm × 1.0 cm × 1.5 cm liver and 1.0 cm distal colon specimens were fixed in 10% buffered formalin for histological examination. Hematoxylin-eosin staining was performed to assess liver steatosis, lobular inflammation, hepatocyte ballooning, inflammation of the colon. Sirius Red staining and Masson's trichrome staining were performed to assess liver fibrosis. Colons were subjected to immunohistochemical staining using specific antibodies for tumor necrosis factor-alpha (TNF-α), 1 beta (IL-1β), C-C motif chemokine ligand 2 (CCL2), and F4/80 (Servicebio, Wuhan, China). TUNEL immunofluorescent staining was performed using a commercially available assay kit (Servicebio, Wuhan, China).

The nonalcoholic fatty liver disease activity score (NAS)[24] and histopathological scoring for intestinal inflammation[25] were evaluated in a blind manner. Steatosis was scored from 0 to 3 based on the quantities of lipid droplets (0, <5%; 1, 5–33%; 2, 34–66%; 3, >66%). Lobular inflammation was scored from 0 to 3 based on the number of inflammatory foci in each 20 × field (0, none; 1, <2 foci; 2, 2–4 foci; 3, >4 foci). Ballooning was scored from 0 to 2 (0, none; 1, few balloon cells; 2, many cells/prominent ballooning). The

intestinal inflammation index was the sum of the scores of colonic epithelial damage (0, normal; 1 hyperproliferation, irregular crypts, goblet cell loss; 2, mild to moderate crypt loss (10–50%); 3, severe crypt loss (50–90%); 4, complete crypt loss, surface epithelium intact; 5, ulcer (<10 crypt widths); 6, large ulcer (≥10 crypt widths), and infiltration with inflammatory cells [mucosa (0–3), submucosa (0–2), and muscle/serosa (0–1)].

For this study, the working definition for NASH was the concurrence of steatosis, lobular inflammation and ballooning or a NAS score ≥5 with the ballooning score ≥1. The successful modeling of UC was comprehensively evaluated by DAI, colon length, and the histopathological scoring for intestinal inflammation. Mice with DAI ≥1, histopathological score ≥1, and a shortened colon were considered UC.

### Statistical analysis

Data were reported as means ± the standard error of the mean (SEM) for each group and were analyzed using Graph-Pad Prism software (v. 8.0.1; GraphPad Software, La Jolla, CA, USA). To compare values obtained from two groups, the Student *t*-test was performed. For three or more groups, one-way analysis of variance followed by a Tukey's multiple comparison test was used. *P*-values of <0.05 were considered significant.

## Results

### Combination of NASH and UC had high mortality in mice

The basic overview of the experimental design in Figure 1 shows that the first half of our study was the 12-week HFHCD-induced NASH model. Mice under HFHCD treatment for 12 weeks had significantly increased body weight, compared with mice on the chow diet (Fig. 2A, B). All mice in the HFHCD group achieved an NAS ≥3, hence they were all considered to have NASH. Specifically, the HFHCD group had a significantly higher steatosis, lobular inflammation, and ballooning scores than the chow diet group (Fig. 2C). After 12 weeks of a chow diet or HFHCD, mice entered the second phase of modeling and started to receive 2% DSS drinking water or normal drinking water. As shown in Figure 2D, DSS dramatically reduced mouse body weight during the first round of treatment in either normal or NASH animals (colitis and steatohepatitis + colitis groups), and to a lesser extent during the next two rounds. Interestingly, throughout the study, the steatohepatitis + colitis group was the only experimental group with mortality (Fig. 2E). The first death occurred soon after the first round of DSS treatment and the final mortality rate was 58.3%, with seven out of the 12 mice in the group dying during the study. Postmortem analysis revealed that rectal bleeding was the predominant cause of death and that one mouse died of multiple organ bleeding.

### UC had mild effects on NASH phenotypes of mice

The mice were euthanized for sample collection at week 20, which was the end of the study. Representative images of liver tissue from the four groups of mice are shown in Figure 2F. Mice in the steatohepatitis + colitis group had a significantly lower body weight and higher liver index than mice in the steatohepatitis group (Fig. 3A). Furthermore, results of the NMR evaluation of body mass composition found that

DSS treatment reduced the ratio of fat to body weight in mice who received the chow diet (control vs. colitis), but not in mice fed the HFHCD (steatohepatitis vs. steatohepatitis + colitis). Mice in the steatohepatitis + colitis group had a significantly lower lean body weight ratio compared with the colitis group, which reflects an additive effect of HFHCD and DSS on consuming lean body weight (Fig. 3B). HFHCD successfully induced mouse liver injury as indicated by increased ALT and AST levels, but we did not observe any influence of DSS treatment (Fig. 3C).

The steatohepatitis + colitis group had increased plasma triglycerides compared with the steatohepatitis group. Whether or not mice received DSS treatment, HFHCD led to increased plasma cholesterol compared with the chow diet (steatohepatitis vs. control and steatohepatitis + colitis vs. colitis). The steatohepatitis + colitis group had the highest plasma cholesterol level of all the experimental groups (Fig. 3D). DSS treatment also decreased hepatic triglyceride levels in when given with both the chow and HFHCD diets without influencing hepatic cholesterol levels (Fig. 3E).

Their disease activity scores confirmed that mice in both the steatohepatitis group and the steatohepatitis + colitis group showed obvious steatohepatitis phenotypes with no differences between the NAS in each group (Fig. 4A, B). Sirius Red staining showed obvious fibrosis in both the steatohepatitis group and the steatohepatitis + colitis group (Fig. 4C). LPS assays in liver homogenates found that the colitis group had a higher hepatic endotoxin level than the chow diet group and that the steatohepatitis + colitis group had a higher hepatic endotoxin level than the steatohepatitis group. No difference was observed between the colitis group and the steatohepatitis group (Fig. 4D). Assay of the hepatic transcriptional levels of *Tnfa*, *f4/80*, *Ccl2*, and *Il1b*, several common markers of liver inflammation were consistent with the histology results. Both the steatohepatitis group and the steatohepatitis + colitis group had up-regulated expressions of *Tnfa*, *f4/80*, and *Il1b*, but there were no differences between the two groups. Surprisingly, hepatic expression of *Ccl2*, the most important chemokine for monocytes/macrophages, was significantly improved in the steatohepatitis + colitis group, compared with the other three groups (Fig. 4E).

### Premorbid NASH exacerbated UC in mice

As no marked gut injury was observed in the control group or the steatohepatitis group (DAI data not shown), we next focused more on the two groups of mice that received DSS treatment for further analyses regarding intestinal injury and inflammation. Colitis severity was evaluated by DAI scores during three rounds of DSS treatment. Mice that received double modeling showed a trend of higher DAI than mice with UC modeling alone. Specifically, the steatohepatitis + colitis group had a higher DAI score on day 7 of the first DSS treatment period (Fig. 5A). Colon samples harvested after three rounds of DSS treatment revealed that mice in the steatohepatitis + colitis group had obviously shorter and more congestive colons than those in the colitis group (Fig. 5B). Mice in the steatohepatitis group did not have clear symptoms of intestinal injury when receiving normal drinking water (i.e., no clear weight loss, rectal bleeding, or stool abnormality, data not shown), their colon length and weight/length ratio were comparable to those of the control group. The colitis group had remarkably shorter colon length, greater colon weight, colon weight/length ratio, and colon weight/body weight ratio, which indicated establishment of the UC model (Fig. 5C). Hematoxylin-eosin staining results showed that premorbid NASH exacerbated DSS-induced gut injury in mice, as significantly higher his-
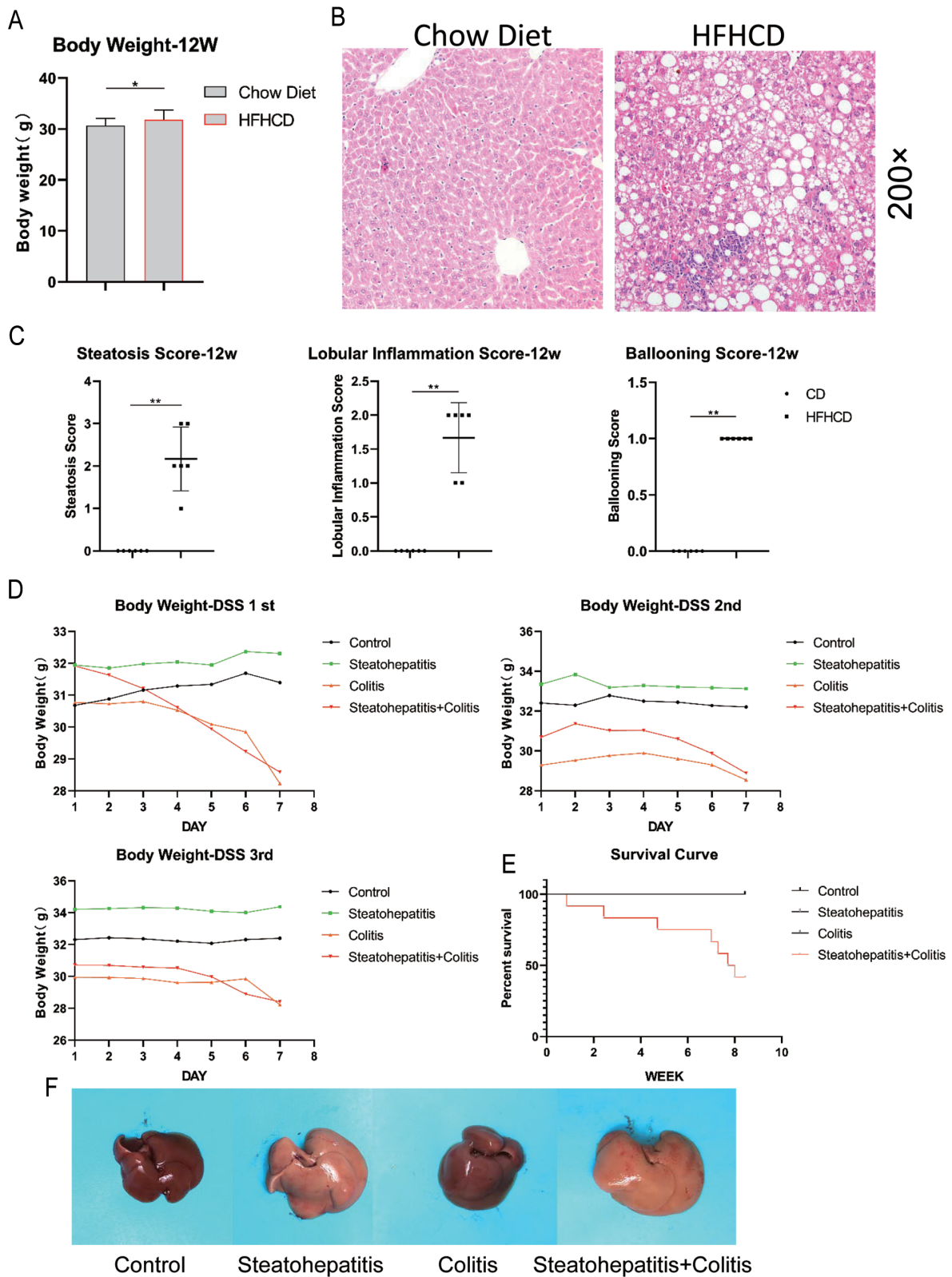
**Fig. 2. The combination of NASH and UC led to significant weight loss and high mortality in mice.** (A) Body weight and (B, C) histological features of 12 weeks of NASH modeling. (D) DSS treatment significantly reduced mouse body weight in both control and NASH mice. (E) The combination of NASH and UC led to high mortality. (F) Images of freshly harvested mouse livers. *$p<0.05$, **$p<0.01$. NASH, nonalcoholic steatohepatitis; UC, ulcerative colitis.
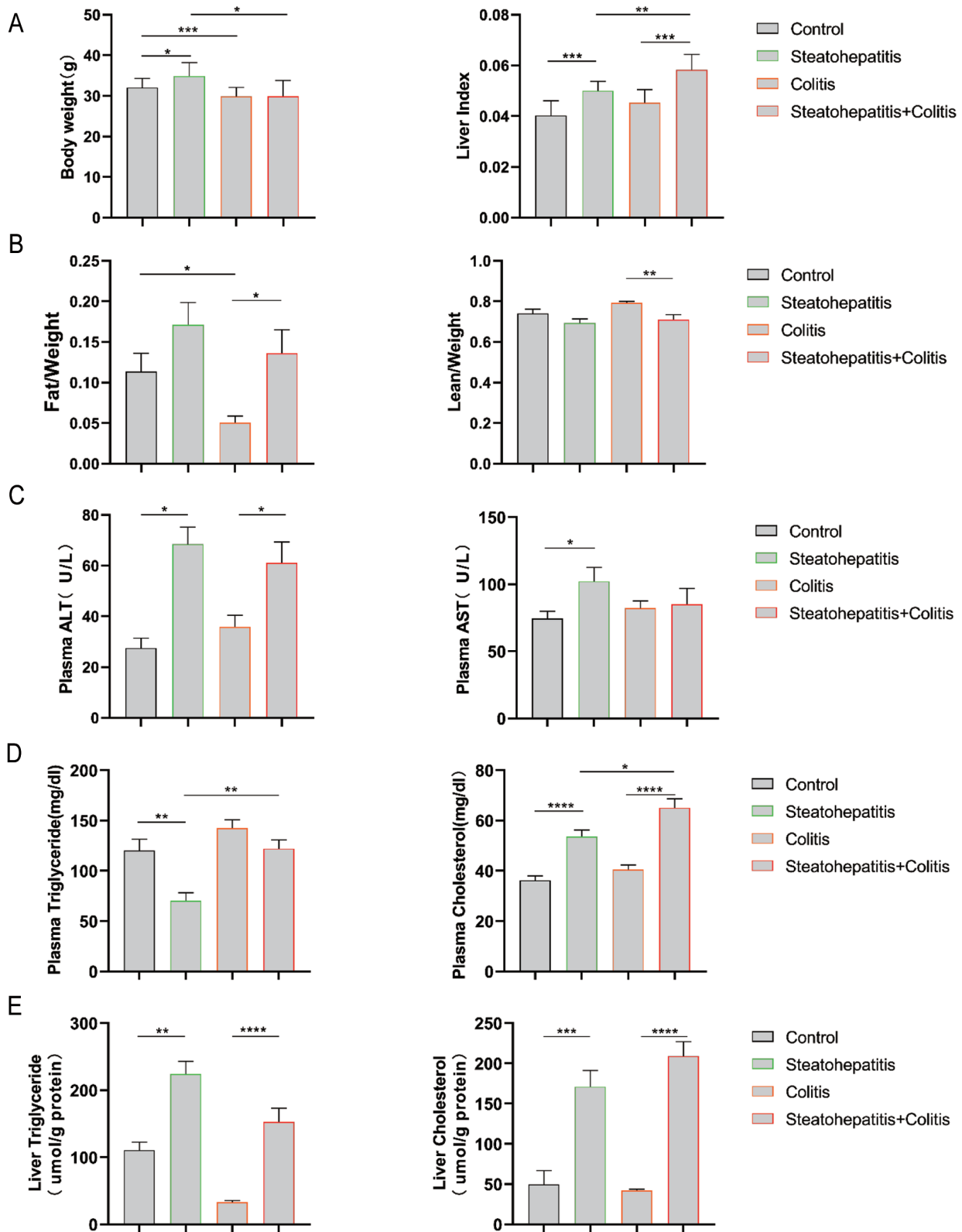
**Fig. 3. NASH-related phenotypes.** Mice received 20 weeks of combined NASH and UC modeling. (A) body weight and liver index. (B) Relative fat body weight and lean body weight. (C) Liver injury indicated by ALT and AST. (D, E) Plasma and hepatic triglyceride and cholesterol levels. *$p<0.05$, **$p<0.01$, ***$p<0.001$. ALT, aminotransferase; AST, aspartate aminotransferase; NASH: nonalcoholic steatohepatitis; UC: ulcerative colitis.
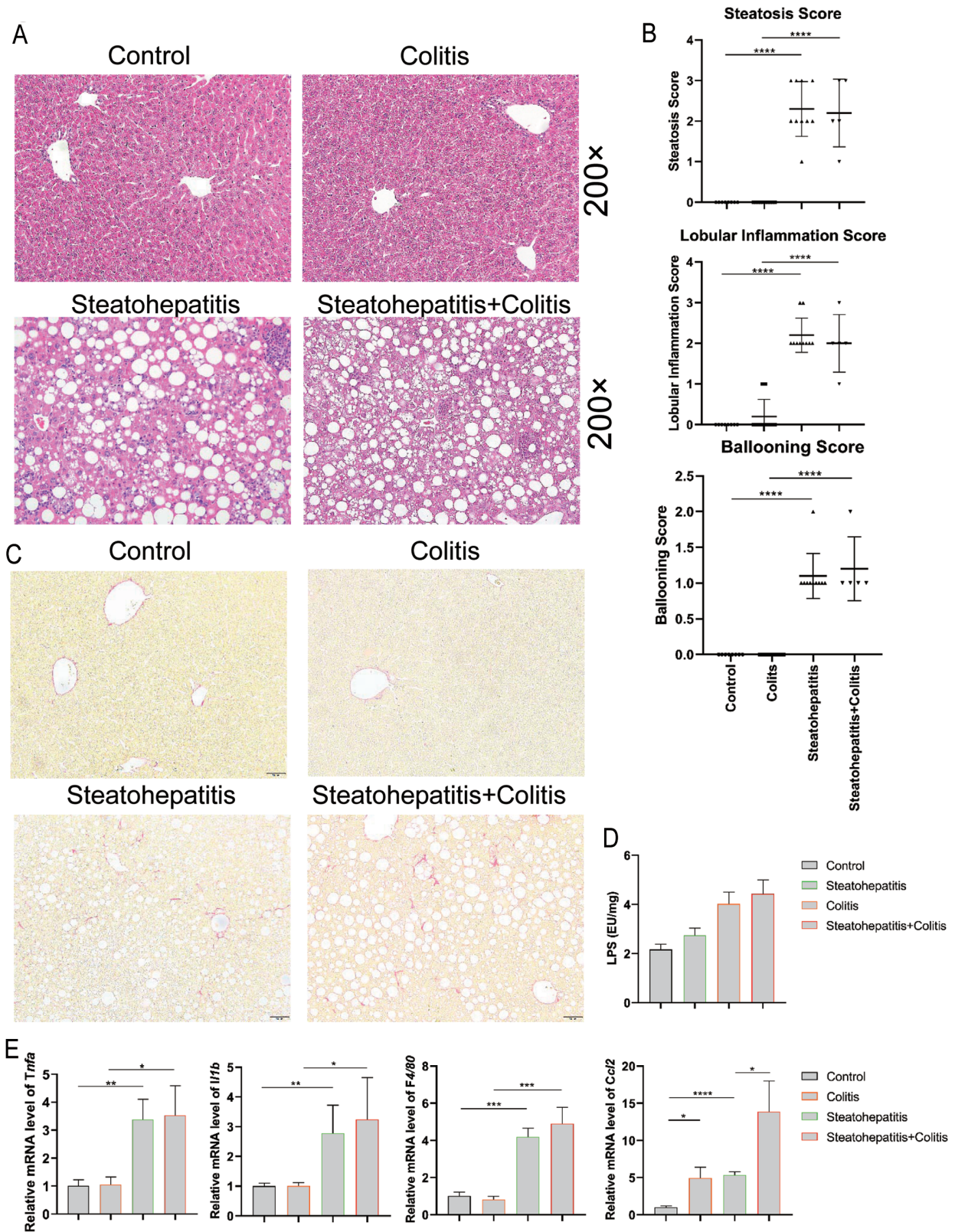
**Fig. 4. Liver injury and inflammation.** Liver samples were harvested from each group of mice for further analysis. (A) Representative HE staining of each group. (B) Corresponding histopathological scores. (C) Representative Sirius Red staining of each group. (D) Hepatic LPS level of each group. (E) Relative mRNA expression of key inflammatory markers. *$p<0.05$, **$p<0.01$, ***$p<0.001$. HE, hematoxylin-eosin; LPS, lipopolysaccharide
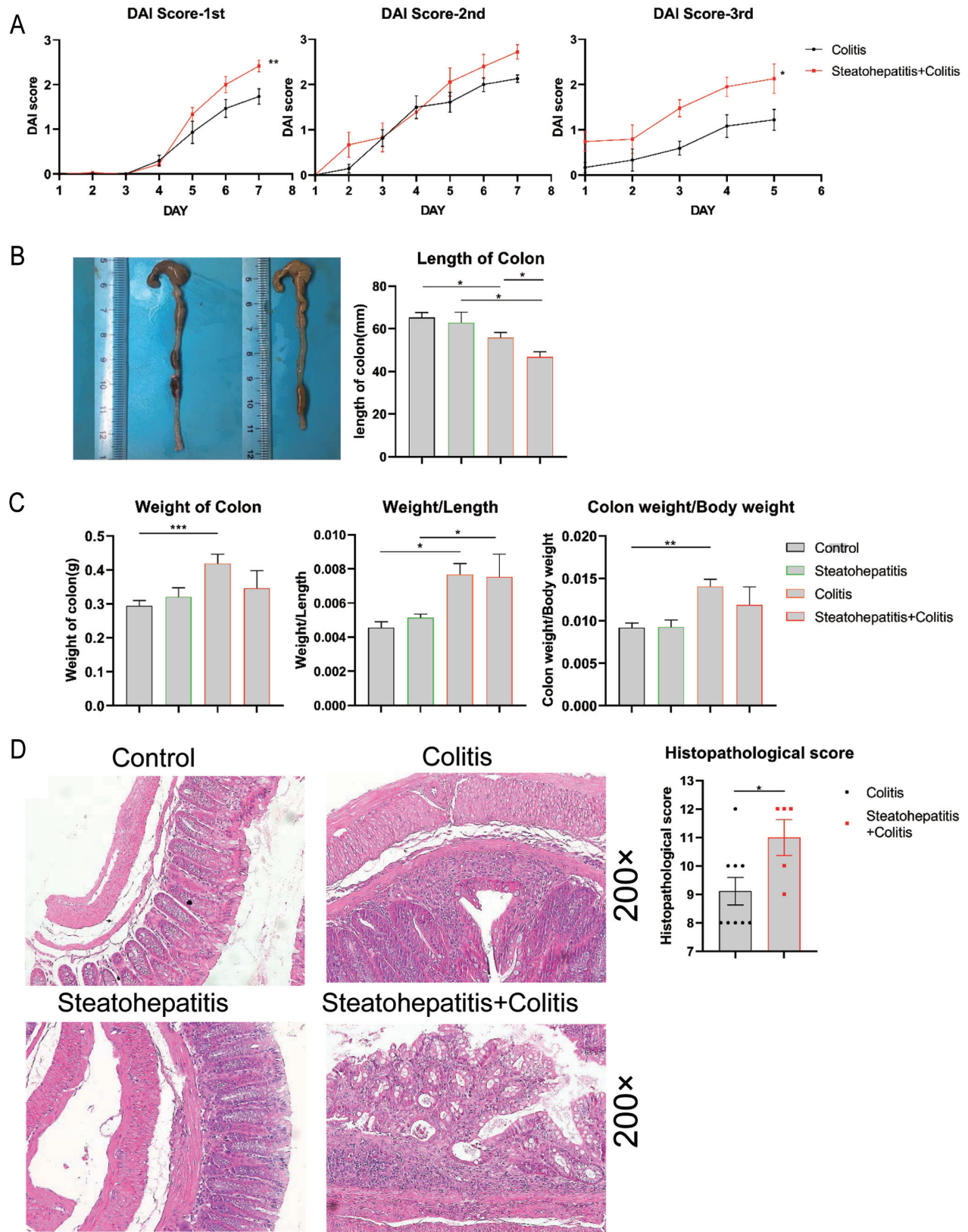
**Fig. 5. UC-related phenotypes of the combined model.** (A) Colitis severity indicated by DAI score. (B) Colon length. (C) Relative colon weight. (D) Representative HE staining and corresponding histopathological score. *$p<0.05$, **$p<0.01$, ***$p<0.001$. DAI, disease activity index; HE, hematoxylin-eosin.
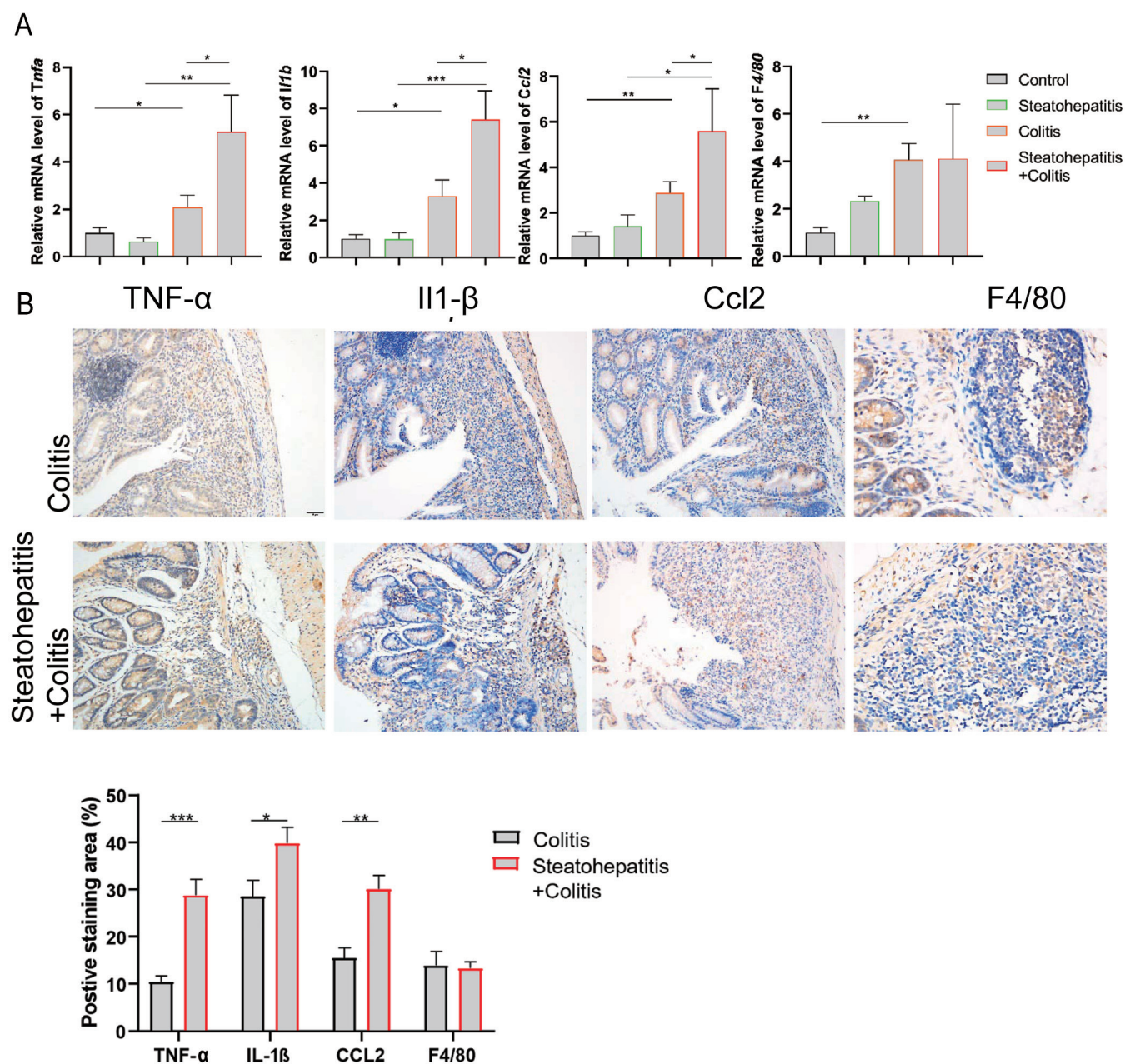
**Fig. 6. Premorbid NASH exacerbated colon injury and inflammation of UC.** (A) Relative mRNA expression of key inflammatory markers in colon tissue. (B) Representative IHC staining and quantification of the positive staining area. IHC, immunohistochemical staining; NASH, nonalcoholic steatohepatitis; UC, ulcerative colitis.

topathology scores was noted in the steatohepatitis + colitis group than in the colitis group (Fig. 5D).

### Premorbid NASH promoted DSS-induced colitis via enhancement of colonic inflammation and injury

In our model, DSS treatment significantly elevated colon expression of *Tnfa* in mice fed the chow diet (colitis vs. control) and premorbid NASH further boosted *Tnfa* mRNA expression in the steatohepatitis + colitis group compared with the colitis group (Fig. 6A). Correspondingly, the combination of NASH and UC synergistically upregulated the expression of *Il1b* and *Ccl2* in the colon (steatohepatitis + colitis vs. colitis). Immunohistochemical staining confirmed a similar trend in the protein expression of the proinflammatory cytokines in the colon. The expression of TNF-α, interleukin 1 beta, and C-C motif chemokine ligand 2 proteins in colon tissue from the steatohepatitis + colitis group was elevated compared with the colitis group (Fig. 6B). Western blot results showed that steatohepatitis + colitis modeling induced the highest expression of NF-κB and Bax of all the study groups, which implies salient inflammatory responses and increased pre-apoptotic signaling (Fig. 7A).

The expression of key apoptotic markers in mouse colon tissues indicated that DSS-induced colitis was associated
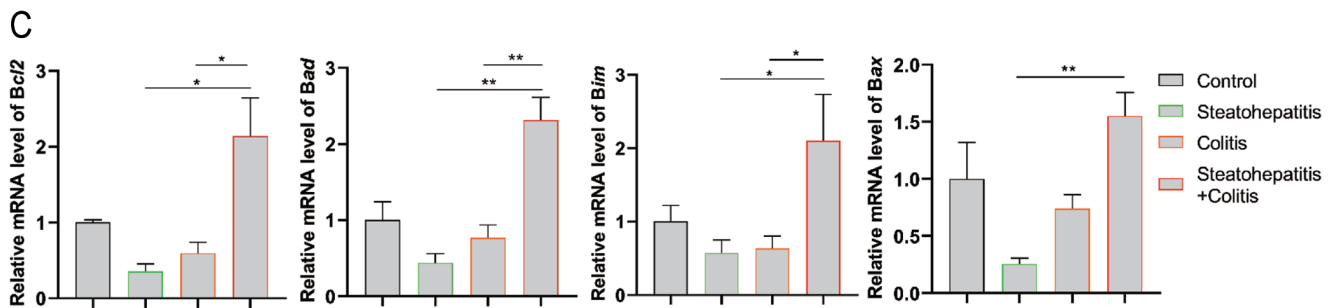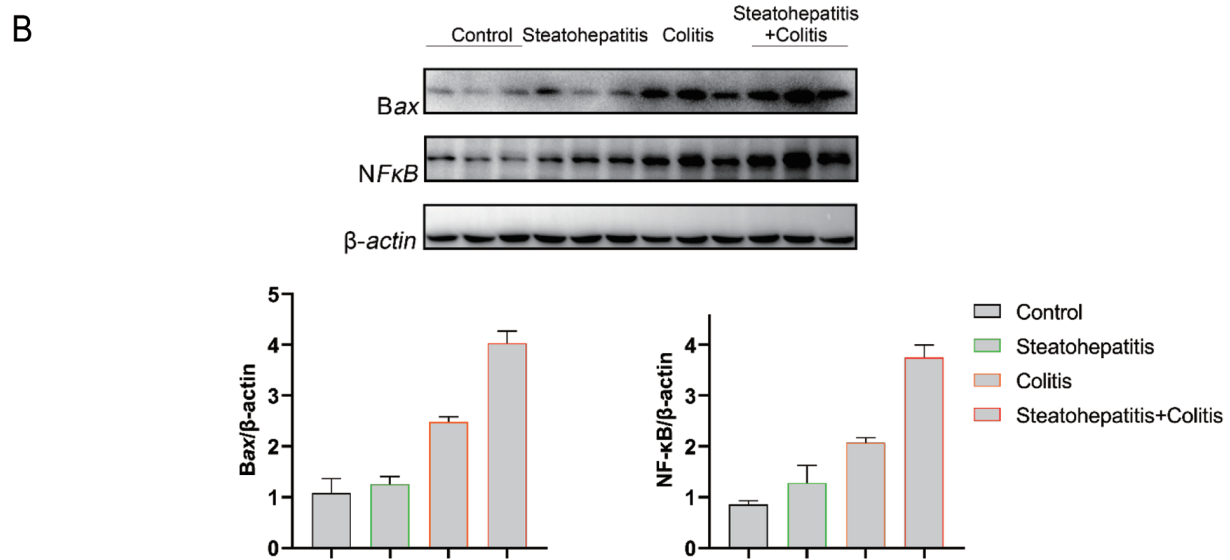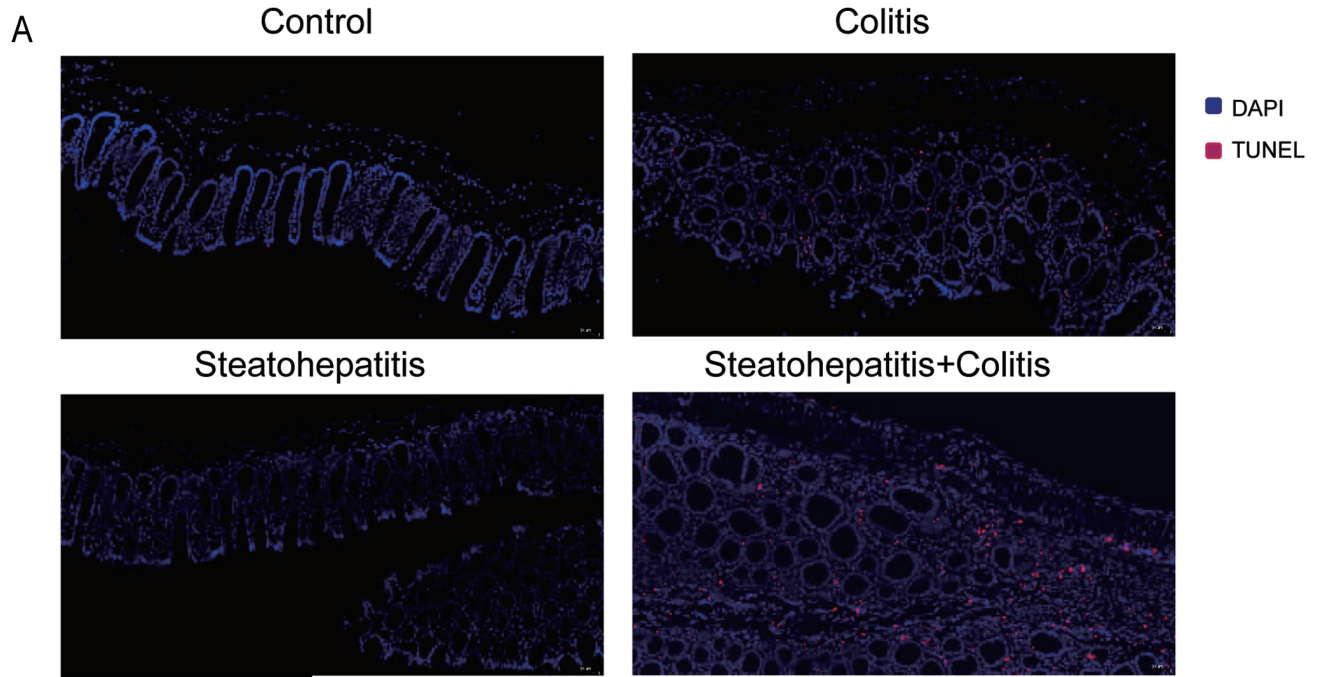
**Fig. 7. Premorbid NASH disturbed colon inflammatory and apoptotic pathways in UC.** (A) Western blots of the relative expression of NF-κB and BAX in colon tissue. (B) Relative mRNA expression of apoptosis signaling. NASH, nonalcoholic steatohepatitis; NF-κB, nuclear factor kappa B; UC, ulcerative colitis.

with maladjusted apoptosis signaling. Colon tissue from the steatohepatitis + colitis group had higher *Bcl2*, *Bad*, *Bim* and *Bax* mRNA levels than either the steatohepatitis group or the colitis group (Fig. 7B).

## Discussion

In this study, we introduced a novel mouse model combining NASH and UC, using HFHCD and DSS. The 12-week HFHCD-induced NASH model was demonstrated to be valid by to their hepatic histological manifestations. Mice that received HFHCD for 12 weeks had prominent liver steatosis, lobular inflammation, and hepatocyte ballooning compared with controls. At the same time, DSS-induced UC was successfully achieved in mice fed with either a chow diet or an HFHCD, as they showed representative symptoms (weight loss, diarrhea and rectal bleeding), colon morphological changes, and histological changes. To our surprise, combination of the two models in the steatohepatitis + colitis group led to fairly high mortality (58.3%), which was present in neither the steatohepatitis group nor the colitis group. Postmortem evaluation found that rectal bleeding was the major cause of death in the mice. The high mortality of the steatohepatitis + colitis group led us to consider whether DSS-induced UC and relevant gut injury were exacerbated by premorbid NASH, which turned out to be the second key study finding. By analyzing distal colon tissues harvested from the DSS group and the steatohepatitis + colitis group, we found that premorbid NASH aggravated UC most likely by facilitating colonic inflammation and apoptosis. Thirdly, we did not observe obvious additive effects of DSS-induced UC on hepatic histological features of NASH. However, DSS treatment caused significant weight loss in both chow diet and HFHCD-fed mice (colitis vs. control and steatohepatitis + colitis vs. steatohepatitis), which successfully mimics the consumptive symptom of UC and flares. Given that the steatohepatitis group had a higher body weight than the control group and the body weight of the steatohepatitis + colitis group was similar to that of the colitis group, UC modeling induced body weight loss was speculated to be more severe in mice with premorbid NASH than in normal mice. Moreover, the steatohepatitis + colitis group had a greater liver weight (as indicated by liver index) than the steatohepatitis group, despite having a lower body weight. This polarized phenomenon indicated that DSS treatment led to mouse emaciation without obviously interfering with liver weight. In other words, exacerbated gut injury and subsequent malabsorption and diarrhea in the steatohepatitis + colitis group may have been the dominant cause of high mortality, while weight loss was the main manifestation.

Recent advances in animal models of NASH[26,27] and UC[28,29] have created convenience for researches aiming not only disease pathogenesis but also therapeutic targets. Because currently available animal models have not yet completely satisfied the need to perfectly simulate both diseases, a new problem has arisen. Recent clinical studies increasingly recognized the concurrence of NASH and UC in patients.[30–32] However, it should be emphasized that the reported associations do not prove causation. In front of us is a "chicken and egg" situation in which NASH may create an inflammatory environment with a leaky gut phenomenon that exacerbates UC, and vice versa. There are several recognized similarities between in disease mechanisms of UC and NASH, such as systematic inflammation, association with obesity, and gut dysbiosis.[33,34] It is apparent that situation necessitates the development of a novel hybrid model integrating NASH and UC for the exploration of underlying disease mechanisms from beside to bench, and back again. It is worth mentioning that we chose a different point to analyze the additive

effects of two diseases compared with former studies, where diet-induced hepatic steatosis was augmented by the synchronized DSS treatment via leaky gut and subsequent lipid dysregulation.[13,35,36] In this study, mice were subjected to long-term HFHCD feeding for NAFLD/NASH modeling and then challenged with three rounds of DSS to mimic the flares of UC. Both real-world NAFLD and UC have heterogeneous phenotypes, hence we fed mice an HFHCD first for NAFLD development and environmental factor-mediated intestinal/systematic low-grade inflammation, before challenging them with unnatural, DSS-induced, intensive chemical injury.

The most distinguishing feature of our hybrid model was the over 50% mortality, similar to observations of UC patients before 1955, when corticosteroids were not available in clinical practice.[4] Simultaneous DSS treatment of mice that ate a chow diet-induced UC in our study, but failed to provoke fulminant and fatal UC flares. Here, premorbid NASH promoted severe UC. As discussed in a recent meta-analysis, NAFLD was more frequent in patients with severe UC, such as longer disease duration or a history of abdominal surgery.[9] Because evidence from cross-sectional studies lacks the ability to prove causality, the finding is partially in agreement with our model, in which severe intestinal injury coexisted with NAFLD. With regard to the lack of a significant difference in the liver histology of tissue from the steatohepatitis group and the steatohepatitis + colitis group in this study, a recent study reported a low risk of liver disease progression in IBD patients with NAFLD.[30] It deserves mention that the steatohepatitis + colitis group had significantly higher plasma triglycerides and cholesterol levels than the steatohepatitis group, and the cause of the phenotype difference needs further study.

TNF-α is one of the most prevalent proinflammatory cytokines in UC, and the benefits of anti-TNF treatment have already been described.[37,38] Altered apoptosis balance has been described in UC and many therapeutic interventions have been developed to modulate colonic apoptotic signaling.[39,40] Thus, some pilot investigations regarding the transcriptional changes of key molecules were carried out to check whether the deteriorated gut injury in the steatohepatitis + colitis group implicates the perturbation of inflammation homeostasis and dysregulation of programmed death. According to our result, NASH mice were more vulnerable to UC gut injury and exhibited significantly upregulated proinflammatory and apoptotic signaling. Given the high prevalence of obesity and NAFLD worldwide nowadays,[41] the current study not merely provides a model of high clinical relevance but also reminds us that NASH people overlapping with UC, not rare as described above, should be wise to prepare for the risk of dire UC flares. But then again, how the liver and gut communicate and work synergistically in this scenario still needs further elucidation. In our future study, individual variate that may contribute the phenotype, such as dietary cholesterol, dietary fat, etc., should be probed one by one.

The study has some limitations. First, high mortality of the combined NASH+UC modeling was speculated as the result of exacerbated inflammation and relevant intestinal symptoms such as bleeding and diarrhea. However, how premorbid NAFLD/NASH leads to worse prognosis of UC in mice should be investigated in future studies. Second, the NASH+UC modeling seemed fail to further complicate NASH phenotypes in this study, which is against our hypothesis. One possible explanation may be that the relatively long duration of HFHCD feeding caused remarkable steatohepatitis and masked the relatively short-term influence of DSS-induced gut inflammation on liver. As revealed by the hematological index, the steatohepatitis + colitis group had a significantly higher inflammation level than other groups right after the first DSS challenge. Hence, that time point may be ideal for future mechanistic studies to avoid the

loss of immune responses and sample loss because of high mortality, in late stage of the combined model. Third, steatosis and inflammation, but not fibrosis and liver cancer were observed. UC may contribute underlying fibrogenic or mutagenic factors to liver in over a longer time span. Last but not least, our NASH model is induced by HFHCD plus added cholesterol, and cholesterol itself was found potentially involved in UC pathogenesis.[42,43] The disturbance of cholesterol metabolism and the high dietary cholesterol consumption have been recognized as unique features in Asian NAFLD population (especially in lean NAFLD cohorts). Thus, it would be interesting to utilize different NASH models or to probe into some universal mechanisms behind the reciprocity of NASH and UC.

## Conclusions

To sum up, premorbid NASH markedly deteriorated DSS-induced colitis, indicating a potential link between NAFLD and UC pathogeneses. The combined mouse NASH and UC model can improve our understanding of the overlap of the two diseases and shed light on more purposeful screening of therapeutic targets. The high mortality of the current hybrid provides an approach for the modeling of severe UC with a strong clinical correlation. Whether NASH can exacerbate UC in patients should be verified by epidemiologic studies a and clinical observation.

## Funding

## Conflict of interest

JGF has been an associate editor of *Journal of Clinical and Translational Hepatology* since 2022.The other authors have no conflicts of interest related to this publication.

## Author contributions

Designed the study and revised the paper (JGF). Conducted the study and wrote the paper (TYR). Conducted the study and analyzed the data (MYW, ZXW). Assisted the histological analysis (LJH, ZYZ, RXY, WHG).

## Data sharing statement

The datasets used and analyzed during the current study are available from the corresponding author, upon reasonable request.

## References

[1] Xavier RJ, Podolsky DK. Unravelling the pathogenesis of inflammatory bowel disease. Nature 2007;448:427–434. doi:10.1038/nature06005, PMID:17653185.
[2] Chow DK, Leong RW, Tsoi KK, Ng SS, Leung WK, Wu JC, *et al*. Long-term follow-up of ulcerative colitis in the Chinese population. Am J Gastroenterol 2009;104:647–654. doi:10.1038/ajg.2008.74, PMID:19262521.
[3] Molodecky NA, Soon IS, Rabi DM, Ghali WA, Ferris M, Chernoff G, *et al*. Increasing incidence and prevalence of the inflammatory bowel diseases with time, based on systematic review. Gastroenterology 2012;142:46–54.e42.
doi:10.1053/j.gastro.2011.10.001, PMID:22001864.
[4] Matsuoka K, Kobayashi T, Ueno F, Matsui T, Hirai F, Inoue N, *et al*. Evidence-based clinical practice guidelines for inflammatory bowel disease. J Gastroenterol 2018;53:305–353. doi:10.1007/s00535-018-1439-1, PMID:29429045.
[5] Eisenstein M. Ulcerative colitis: towards remission. Nature 2018;563:S33. doi:10.1038/d41586-018-07276-2, PMID:30405234.
[6] Kobayashi T, Siegmund B, Le Berre C, Wei SC, Ferrante M, Shen B, *et al*. Ulcerative colitis. Nat Rev Dis Primers 2020;6:74. doi:10.1038/s41572-020-0205-x, PMID:32913180.
[7] Kaplan GG. The global burden of IBD: from 2015 to 2025. Nat Rev Gastroenterol Hepatol 2015;12:720–727. doi:10.1038/nrgastro.2015.150, PMID:26323879.
[8] Singh S, Dulai PS, Zarrinpar A, Ramamoorthy S, Sandborn WJ. Obesity in IBD: epidemiology, pathogenesis, disease course and treatment outcomes. Nat Rev Gastroenterol Hepatol 2017;14:110–121. doi:10.1038/nrgastro.2016.181, PMID:27899815.
[9] Zou ZY, Shen B, Fan JG. Systematic Review With Meta-analysis: Epidemiology of Nonalcoholic Fatty Liver Disease in Patients With Inflammatory Bowel Disease. Inflamm Bowel Dis 2019;25:1764–1772. doi:10.1093/ibd/izz043, PMID:30918952.
[10] Tripathi A, Debelius J, Brenner DA, Karin M, Loomba R, Schnabl B, *et al*. The gut-liver axis and the intersection with the microbiome. Nat Rev Gastroenterol Hepatol 2018;15:397–411. doi:10.1038/s41575-018-0011-z, PMID:29748586.
[11] Albillos A, de Gottardi A, Rescigno M. The gut-liver axis in liver disease: Pathophysiological basis for therapy. J Hepatol 2020;72:558–577. doi:10.1016/j.jhep.2019.10.003, PMID:31622696.
[12] Boursier J, Mueller O, Barret M, Machado M, Fizanne L, Araujo-Perez F, *et al*. The severity of nonalcoholic fatty liver disease is associated with gut dysbiosis and shift in the metabolic function of the gut microbiota. Hepatology 2016;63:764–775. doi:10.1002/hep.28356, PMID:26600078.
[13] Cheng C, Tan J, Qian W, Zhang L, Hou X. Gut inflammation exacerbates hepatic injury in the high-fat diet induced NAFLD mouse: Attention to the gut-vascular barrier dysfunction. Life Sci 2018;209:157–166. doi:10.1016/j.lfs.2018.08.017, PMID:30096384.
[14] Dulai PS, Levesque BG, Feagan BG, D'Haens G, Sandborn WJ. Assessment of mucosal healing in inflammatory bowel disease: review. Gastrointest Endosc 2015;82:246–255. doi:10.1016/j.gie.2015.03.1974, PMID:26005012.
[15] Ni J, Wu GD, Albenberg L, Tomov VT. Gut microbiota and IBD: causation or correlation? Nat Rev Gastroenterol Hepatol 2017;14:573–584. doi:10.1038/nrgastro.2017.88, PMID:28743984.
[16] Schirmer M, Garner A, Vlamakis H, Xavier RJ. Microbial genes and pathways in inflammatory bowel disease. Nat Rev Microbiol 2019;17:497–511. doi:10.1038/s41579-019-0213-6, PMID:31249397.
[17] Jiao N, Baker SS, Chapa-Rodriguez A, Liu W, Nugent CA, Tsompana M, *et al*. Suppressed hepatic bile acid signalling despite elevated production of primary and secondary bile acids in NAFLD. Gut 2018;67:1881–1891. doi:10.1136/gutjnl-2017-314307, PMID:28774887.
[18] Hwang S, Ren T, Gao B. Obesity and binge alcohol intake are deadly combination to induce steatohepatitis: A model of high-fat diet and binge ethanol intake. Clin Mol Hepatol 2020;26:586–594. doi:10.3350/cmh.2020.0100, PMID:32937687.
[19] Henao-Mejia J, Elinav E, Jin C, Hao L, Mehal WZ, Strowig T, *et al*. Inflammasome-mediated dysbiosis regulates progression of NAFLD and obesity. Nature 2012;482:179–185. doi:10.1038/nature10809, PMID:22297845.
[20] Zhen Y, Zhang H. NLRP3 Inflammasome and Inflammatory Bowel Disease. Front Immunol 2019;10:276. doi:10.3389/fimmu.2019.00276, PMID:30873162.
[21] Bauer C, Duewell P, Mayer C, Lehr HA, Fitzgerald KA, Dauer M, *et al*. Colitis induced in mice with dextran sulfate sodium (DSS) is mediated by the NLRP3 inflammasome. Gut 2010;59:1192–1199. doi:10.1136/gut.2009.197822, PMID:20442201.
[22] Peng L, Gao X, Nie L, Xie J, Dai T, Shi C, *et al*. Astragalin Attenuates Dextran Sulfate Sodium (DSS)-Induced Acute Experimental Colitis by Alleviating Gut Microbiota Dysbiosis and Inhibiting NF-kappaB Activation in Mice. Front Immunol 2020;11:2058. doi:10.3389/fimmu.2020.02058, PMID:33042117.
[23] Zhou D, Pan Q, Xin FZ, Zhang RN, He CX, Chen GY, *et al*. Sodium butyrate attenuates high-fat diet-induced steatohepatitis in mice by improving gut microbiota and gastrointestinal barrier. World J Gastroenterol 2017;23:60–75. doi:10.3748/wjg.v23.i1.60, PMID:28104981.
[24] Hou Z, Ye Q, Qiu M, Hao Y, Han J, Zeng H. Increased activated regulatory T cells proportion correlate with the severity of idiopathic pulmonary fibrosis. Respir Res 2017;18:170. doi:10.1186/s12931-017-0653-3, PMID:28886713.
[25] Katakura K, Lee J, Rachmilewitz D, Li G, Eckmann L, Raz E. Toll-like receptor 9-induced type I IFN protects mice from experimental colitis. J Clin Invest 2005;115:695–702. doi:10.1172/JCI22996, PMID:15765149.
[26] Santhekadur PK, Kumar DP, Sanyal AJ. Preclinical models of non-alcoholic fatty liver disease. J Hepatol 2018;68:230–237. doi:10.1016/j.jhep.2017.10.031, PMID:29128391.
[27] Farrell G, Schattenberg JM, Leclercq I, Yeh MM, Goldin R, Teoh N, *et al*. Mouse Models of Nonalcoholic Steatohepatitis: Toward Optimization of Their Relevance to Human Nonalcoholic Steatohepatitis. Hepatology 2019;69:2241–2257. doi:10.1002/hep.30333, PMID:30372785.
[28] Nascimento RPD, Machado A, Galvez J, Cazarin CBB, Marostica Junior MR. Ulcerative colitis: Gut microbiota, immunopathogenesis and application of natural products in animal models. Life Sci 2020;258:118129. doi:10.1016/j.lfs.2020.118129, PMID:32717271.

[29] Mizoguchi A. Animal models of inflammatory bowel disease. Prog Mol Biol Transl Sci 2012;105:263–320. doi:10.1016/B978-0-12-394596-9.00009-3, PMID:22137435.

[30] Ritaccio G, Stoleru G, Abutaleb A, Cross RK, Shetty K, Sakiani S, *et al*. Nonalcoholic Fatty Liver Disease Is Common in IBD Patients However Progression to Hepatic Fibrosis by Noninvasive Markers Is Rare. Dig Dis Sci 2021;66:3186–3191. doi:10.1007/s10620-020-06588-6, PMID:32894439.

[31] Magri S, Paduano D, Chicco F, Cingolani A, Farris C, Delogu G, *et al*. Nonalcoholic fatty liver disease in patients with inflammatory bowel disease: Beyond the natural history. World J Gastroenterol 2019;25:5676–5686. doi:10.3748/wjg.v25.i37.5676, PMID:31602167.

[32] Principi M, Iannone A, Losurdo G, Mangia M, Shahini E, Albano F, *et al*. Nonalcoholic Fatty Liver Disease in Inflammatory Bowel Disease: Prevalence and Risk Factors. Inflamm Bowel Dis 2018;24:1589–1596. doi:10.1093/ibd/izy051, PMID:29688336.

[33] Rivas MA, Beaudoin M, Gardet A, Stevens C, Sharma Y, Zhang CK, *et al*. Deep resequencing of GWAS loci identifies independent rare variants associated with inflammatory bowel disease. Nat Genet 2011;43:1066–1073. doi:10.1038/ng.952, PMID:21983784.

[34] Lee D, Albenberg L, Compher C, Baldassano R, Piccoli D, Lewis JD, *et al*. Diet in the pathogenesis and treatment of inflammatory bowel diseases. Gastroenterology 2015;148:1087–1106. doi:10.1053/j.gastro.2015.01.007, PMID:25597840.

[35] Gabele E, Dostert K, Hofmann C, Wiest R, Scholmerich J, Hellerbrand C, *et al*. DSS induced colitis increases portal LPS levels and enhances hepatic inflammation and fibrogenesis in experimental NASH. J Hepatol 2011;55:1391–1399. doi:10.1016/j.jhep.2011.02.035, PMID:21703208.

[36] Kwon J, Lee C, Heo S, Kim B, Hyun CK. DSS-induced colitis is associated with adipose tissue dysfunction and disrupted hepatic lipid metabolism leading to hepatosteatosis and dyslipidemia in mice. Sci Rep 2021;11:5283. doi:10.1038/s41598-021-84761-1, PMID:33674694.

[37] He C, Shi Y, Wu R, Sun M, Fang L, Wu W, *et al*. miR-301a promotes intestinal mucosal inflammation through induction of IL-17A and TNF-alpha in IBD. Gut 2016;65:1938–1950. doi:10.1136/gutjnl-2015-309389, PMID:26338824.

[38] Atreya R, Neurath MF, Siegmund B. Personalizing Treatment in IBD: Hype or Reality in 2020? Can We Predict Response to Anti-TNF? Front Med (Lausanne) 2020;7:517. doi:10.3389/fmed.2020.00517, PMID:32984386.

[39] Kuo WT, Shen L, Zuo L, Shashikanth N, Ong M, Wu L, *et al*. Inflammation-induced Occludin Downregulation Limits Epithelial Apoptosis by Suppressing Caspase-3 Expression. Gastroenterology 2019;157:1323–1337. doi:10.1053/j.gastro.2019.07.058, PMID:31401143.

[40] Pott J, Kabat AM, Maloy KJ. Intestinal Epithelial Cell Autophagy Is Required to Protect against TNF-Induced Apoptosis during Chronic Colitis in Mice. Cell Host Microbe 2018;23:191–202.e194. doi:10.1016/j.chom.2017.12.017, PMID:29358084.

[41] Younossi ZM, Golabi P, de Avila L, Paik JM, Srishord M, Fukui N, *et al*. The global epidemiology of NAFLD and NASH in patients with type 2 diabetes: A systematic review and meta-analysis. J Hepatol 2019;71:793–801. doi:10.1016/j.jhep.2019.06.021, PMID:31279902.

[42] Tan JMJ, Mellouk N, Osborne SE, Ammendolia DA, Dyer DN, Li R, *et al*. An ATG16L1-dependent pathway promotes plasma membrane repair and limits Listeria monocytogenes cell-to-cell spread. Nat Microbiol 2018;3:1472–1485. doi:10.1038/s41564-018-0293-5, PMID:30478389.

[43] Fiorucci S, Carino A, Baldoni M, Santucci L, Costanzi E, Graziosi L, *et al*. Bile Acid Signaling in Inflammatory Bowel Diseases. Dig Dis Sci 2021;66:674–693. doi:10.1007/s10620-020-06715-3, PMID:33289902.